Construction and Building Materials 140 (2017) 310–320

Contents lists available at ScienceDirect

Construction and Building Materials

journal homepage: www.elsevier.com/locate/conbuildmat

The effect of elevated conditioning temperature on the ASR expansion, cracking and properties of reactive Spratt aggregate concrete

Bishnu P. Gautam [a], Daman K. Panesar [b,*]

[a] Sarthak Concrete Pvt. Ltd., Samakhusi, Kathmandu, Nepal
[b] Department of Civil Engineering, University of Toronto, Canada

HIGHLIGHTS

- 12 °C rise in temperature accelerated the expansion by 3.22 times.
- Similar trend of loss in mechanical properties at both temperatures.
- Slightly larger extent of loss and microstructural cracking at 50 °C than at 38 °C.

ARTICLE INFO

Article history:
Received 24 September 2016
Received in revised form 26 January 2017
Accepted 19 February 2017
Available online 3 March 2017

Keywords:
Alkali-silica reaction (ASR)
Temperature
Acceleration
Expansion
Damage rating index
Concrete prism test

ABSTRACT

In the laboratory study of alkali-silica reaction (ASR), attempts have been made to reduce the test duration by accelerating the rate of reaction, which is usually accomplished by increasing the conditioning temperature. However, the consequences of elevating temperature are not so encouraging. This study evaluated the effects of elevated temperature by comparing expansion, damage rating index and mechanical properties of concrete made with Spratt aggregate conditioned at 38 °C and 50 °C. Increasing the temperature to 50 °C from 38 °C can shorten the test duration by more than three times with little effect on the response of concrete.

1. Introduction

Alkali-silica reaction (ASR) is an undesirable chemical reaction in concrete that causes expansion, cracking and degradation of mechanical properties. Even though ASR has now been adequately understood to ensure that new concrete structures are safe against it, ASR is still a major deterioration problem in many existing structures. The rate of reaction is generally slow and usually takes 10 years or more to show its effects in field concrete structures [1]. In an experimental study that involved large concrete specimens subjected to an outdoor condition, ASR expansion was monitored and it continued for 20 years [2]. However, the urgent need for diagnosis, prognosis and necessary repair measures of existing structures cannot afford such a long duration for an experimental study. Therefore, experimental studies on concrete specimens are typically performed under an accelerated condition. While most of the accelerated studies involve small specimens such as concrete prisms (75 × 75 × 285 mm) and cylinders (Ø100 × height 200 mm), the study of larger specimens (1 m or longer) such as beams and walls are preferred to understand the performance of concrete structures affected by ASR [3–5].

The relatively slow rate of ASR is a challenge for evaluating its implications on structural performance. While small specimens can be accommodated in existing laboratory facilities, maintaining the conditions necessary for accelerating the rate of reaction in large structural specimens and conditioning them for an extended duration can be logistically challenging. These are some reasons why large specimens are rarely examined in ASR studies. One such study [3] involved 3 m long concrete beams (cross-section of 0.25 × 0.5 m) that were subjected to an elevated temperature of 38 °C. The measurements in the beams were reported for 14 months. Yet, the increasing expansion and beam deflection indicated that the reaction was not exhausted by the end of the study duration. Relatively larger thickness of the beams, when compared

* Corresponding author at: Department of Civil Engineering, University of Toronto, 35 St. George St., Toronto, Ontario M5S 1A4, Canada.
E-mail addresses: bgautam@gmail.com (B.P. Gautam), d.panesar@utoronto.ca (D.K. Panesar).

http://dx.doi.org/10.1016/j.conbuildmat.2017.02.104
0950-0618/

to the small specimens such as prisms, might have partly contributed to the lengthened duration of the reaction. A laboratory study of large structural specimens necessitates an accelerating condition that fosters a faster rate of reaction.

Accelerating the rate of reaction can be achieved by increasing the exposure temperature, relative humidity, or alkalinity, or combinations thereof. Most laboratory studies employ the combination of all three accelerating measures. Nevertheless, increasing the temperature appears to be the most common accelerating variable to increase the rate of reaction.

The most common temperature for accelerating ASR on concrete specimens is 38 °C based on the concrete prism test (CPT), which is regarded as a reliable reference test method for assessing the potential alkali-silica reactivity of aggregates as per ASTM [6], CSA [7] and RILEM [8] standards. However, the duration of the CPT is 1–2 years and the test is regarded as slow for many purposes. Practical requirements have encouraged to shorten the test duration by further increasing the temperature [9–11]. For instance, the accelerated concrete prism test (ACPT), usually performed at 60 °C [12], has emerged as a faster alternative to CPT. Nevertheless, the 60 °C temperature method is reported to cause reduced expansion compared to that achieved when exposed to 38 °C temperature [13,14]. Some reasons for the reduced expansion at 60 °C are [13,14] (i) increased leaching of alkalies; (ii) change in pore solution chemistry owing to the reduced concentration of hydroxyl ions; and (iii) drying of prisms at higher temperature. Another unusual observation reported in the study [14] of ASR conducted at 60 °C was that non-reactive fine aggregate had a "dramatic effect" on reducing the expansion and increasing the variability in expansion measurements [14].

Considering the complexity associated with interpretation of the response of ASR-affected concrete specimens conditioned at 60 °C, Folliard et al. [13] performed a series of concrete prism tests at 49 °C, which is an intermediate value between 38 and 60 °C. While the ultimate expansion decreased with an increase in temperature, this effect was more pronounced for the temperature increment from 49 to 60 °C than from 38 to 49 °C. The ultimate expansions corresponding to 60 °C (0.09%) were markedly less than those corresponding to 49 °C (0.17%) and 38 °C (0.20%). A non-linear effect of the two temperature increments was also observed in terms of alkali leaching. Alkali leaching was more pronounced for the temperature increment from 49 to 60 °C than from 38 to 49 °C. These findings indicate that the accelerating temperature for investigating the performance of large specimens should be limited to around 50 °C.

An increase in temperature accelerates the rate of ASR by thermoactivating two processes involved in ASR [15]. Firstly, an increase in temperature accelerates the dissolution of silica in aggregates. For instance, the rates of dissolution of three types of silica particles measured at 25 °C in 3 M NaOH solution for 3 days were 71%, 8% and 7%, whereas these amounts were, respectively, 100%, 66% and 31% when measured at 80 °C [16]. In another study [17], the dissolution of silica at 80 °C was reported to be 6–7 times more than at 60 °C. Secondly, increased temperature accelerates the rate of formation of reaction products [15]. Results from an experimental study [18] on concrete conditioned at temperatures ranging from 23 to 58 °C confirmed that both processes follow the Arrhenius law of chemical reaction [15]. Based on the formulas for two time constants for the two processes [15], the rate of expansion is approximately doubled when the temperature is increased from 38 to 50 °C. As per the formulas proposed in another experimental study [19], the rate of reaction can be increased by approximately 1.7 times when the temperature is increased from 38 to 50 °C. These findings indicate that the test duration can be significantly reduced by choosing 50 °C instead of 38 °C as the accelerating temperature for large concrete specimens.

Recently, an accelerating temperature of 50 °C was chosen in a large-scale project aimed at investigating the consequences of ASR on existing structures [20]. The project involved several large unreinforced and reinforced concrete specimens with thickness ranging from 75 to 254 mm and length of up to 1.5 m. Even though the accelerating temperature was 50 °C, the study had to rely on the vast knowledge of ASR gained mainly through experiments performed at 38 °C. For example, the reactivity of aggregate to be used for casting the specimens was decided based on the expansion of concrete prisms tested at 38 °C. To evaluate the effect of temperature increment from 38 to 50 °C on expansion, which is one of the key performance indicators for reactive concrete, a study was necessary to compare the expansion results at the two temperatures. Moreover, the specimens were designed to be monitored for the performance of concrete in terms of cracking and degradation of mechanical properties. However, most of the performance indicators for ASR damage are either unavailable or inadequate for tests at 50 °C. The damage rating index (DRI) is one such indicator that quantitatively assesses the damage due to ASR based mainly on the cracks it develops in concrete. The DRI method has been extensively applied on field samples and on specimens conditioned at 38 °C [21–24]. In order to assess DRI as a performance indicator for ASR-affected concrete, Sanchez [25] performed DRI analysis of twenty concrete mixtures made with a variety of reactive aggregates. The study discussed the influence of concrete strength and different types of reactive aggregates on DRI. However, all the experiments were performed at 38 °C, and hence, the effect of temperature on damage was not investigated. An increase in temperature can lead to greater damage despite having identical ultimate expansion as indicated by a recent numerical study [26]. While expansion mainly depends on the amount of reaction product formed and not on its rate of formation, microstructural damage is influenced by the creep effect which in turn is influenced by the rate of reaction [26]. Thus, a study comparing DRI of identical concrete specimens conditioned at 38 °C and at 50 °C is essential before DRI can be used as a performance indicator for the concrete specimens conditioned at 50 °C. Furthermore, to better understand the influence of increasing temperature on the damage of concrete, the degradation of mechanical properties should be compared at the two temperatures.

This paper compares the consequences of ASR on identical concrete prism specimens conditioned at 38 °C and at 50 °C. Both test sets (one at 38 °C and the other at 50 °C) include reactive and non-reactive (control) mixes of concrete. Longitudinal expansion of the prism specimens from the two tests is compared. Prism specimens from the two tests are analyzed by the DRI method. The results are discussed to compare the damage between the two tests, to elucidate the evolution of ASR damage, and also to highlight some limitations of the DRI method. The degradation of dynamic modulus of elasticity and modulus of rupture of the prism specimens is measured. Based on the findings from the tests, a conclusion is made regarding the implication of increasing the accelerating temperature from 38 to 50 °C.

2. Materials and methods

2.1. Concrete mix design and materials

The mix design was based on the concrete prism test as per ASTM C1293 [6], and is shown in Table 1. The water-to-cement ratio was 0.44. High alkali general use (GU) cement was used with a total alkali content of 0.99% Na_2O equivalent by mass of cement. The chemical composition of cement is shown in Table 2. The alkali

Table 1
Mix design of concrete.

Mix	Cement (kg/m^3)	Water (kg/m^3)	Coarse aggregate (kg/m^3)	Sand (kg/m^3)	Alkali pellets (kg/m^3)
Reactive	420	184.8	1115.0	719.2	1.41
Control	420	184.8	1138.8	691.0	1.41

Note: The dry-rodded density of reactive coarse aggregate was 1585 kg/m^3 and that of non-reactive coarse aggregate was 1604 kg/m^3.
The mass of aggregates is shown for saturated surface-dry condition.

Table 2
Chemical composition of GU cement.

Constituents	Loss on ignition	SiO_2	Al_2O_3	Fe_2O_3	CaO	MgO	SO_3	Total alkali (Na_2O_{eq})	Free lime	Insoluble residue
Percentage (by mass)	2.27	19.25	5.33	2.41	62.78	2.36	4.01	0.99	1.29	0.52

content of the mix was boosted to 1.25% Na_2O equivalent by adding reagent grade NaOH pellets to water prior to concrete mixing. No other admixtures were used.

Two types of concrete were considered, namely reactive and non-reactive (control). The reactive concrete was made with reactive coarse aggregate and non-reactive fine aggregate. The control concrete consisted of non-reactive fine and non-reactive coarse aggregates. The non-reactive coarse aggregate for the control concrete was crushed limestone aggregate from Milton, Ontario, Canada. Non-reactive fine aggregate was natural sand from Orillia, Ontario, Canada. An accelerated mortar bar test was performed to confirm the non-reactivity of sand as per ASTM C1260 [27].

The reactive coarse aggregate was Spratt aggregate from a quarry in Stittsville near Ottawa, Ontario, Canada [28]. The siliceous limestone containing reactive silica minerals (9% SiO_2 [2]) is classified as highly reactive aggregate, and has been used as the most popular reference aggregate to calibrate ASR test methods [28–30]. Except for ASR, the aggregate meets the physical requirements for concrete aggregate [2]. The Los Angeles Abrasion value for Spratt aggregate was reported as 19% [31]. The specific gravity of the aggregate at oven-dry condition was 2.68 and the absorption was 0.5%.

2.2. Casting and conditioning of the specimens

2.2.1. Concrete prism specimens conditioned at 38 °C (CPT)

The first set of tests performed on concrete prisms conditioned at 38 ± 2 °C is referred to as the concrete prism test (CPT) in this study. Concrete prisms were cast as per ASTM C1293 [6]. Eighteen reactive and twelve control prisms were cast. The size of the prism specimens was 285 mm × 75 mm × 75 mm. Initial reading for longitudinal expansion was taken after demolding at one day of casting. The specimens were stored in sealed plastic pails in the vertical orientation and flipped at successive measurement intervals. Since the day of demolding, the prisms were cured under a constant temperature of 38 ± 2 °C and relative humidity > 95%. The humidity was maintained by having a water layer at the bottom of the pails that was separated by an air space from the bottom end of the prisms. The pails were lined with a layer of water absorbent paper that dipped to the bottom of the pail. Tests on the specimens were performed at the ages of 7, 28, 56, 91, 182, 273, 365 and 730 days. All test measurements were taken at room temperature by acclimatizing the pails beforehand for 16–20 h.

2.2.2. Concrete prism specimens conditioned at 50 °C (ACPT)

The second set of tests was performed on concrete prisms conditioned at 50 ± 0.5 °C and is referred to as the accelerated concrete prism test (ACPT) in this study. Nine concrete prisms were cast for each of the reactive and the control mixes. The specimen casting, demolding and initial measurements were similar to those mentioned in Section 2.2.1. Upon demolding the specimens, pails containing three prism specimens each were stored at a constant temperature of 50 ± 0.5 °C. The relative humidity (>95%) was maintained by the method detailed in Section 2.2.1. Furthermore, the pails were stored inside a large acceleration chamber which was maintained at >95% relative humidity. Tests on the specimens were performed at the ages of 7, 28, 56, 91, 127, 159 and 187 days. All test measurements were taken at room temperature by acclimatizing the specimens in the pails beforehand for 16–20 h.

2.3. Test details

2.3.1. Expansion measurement

Longitudinal expansion was measured on the concrete prisms. The expansion was measured using a comparator against the steel studs embedded in the ends of the prisms with a gauge length of 250 mm. The comparator has a resolution of 1 μm, and was calibrated with a reference invar bar. The expansion at a given age was calculated as the difference between the comparator reading at the given age and the initial comparator reading taken at the day of demolding.

2.3.2. Modulus of rupture

Two prisms were tested by third-point loading as outlined in ASTM C78 [32]. The span length (L) was maintained as 225 mm, which is three times the depth of the prism (d = 75 mm).

The modulus of rupture (R) (MPa) was calculated as,

$$R = \frac{PL}{bd^2} \quad (1)$$

where P (N) is the maximum applied load and b (mm) is the average width of the prism. The values of b and d (mm) used in the calculation were taken by measuring each prism with a caliper.

The fracture always occurred in the tension surface within the middle third of the span. The cracked middle portion of the prisms was discarded while the remaining portion of the prism was utilized for DRI analysis as described in Section 2.3.5.

2.3.3. Transverse resonant frequency

Fundamental transverse resonant frequency of the prisms was measured as per ASTM C215 [33], as a non-destructive method of estimating the degradation of dynamic modulus of elasticity of the prisms. A test prism was supported at its two nodal points located at a distance of 0.224 times the length of the prism from either end of the prism. The resonant frequency was observed as the maximum frequency obtained by changing the frequency of the driving force until resonance would occur. Dynamic modulus of elasticity (E_d) (Pa) was calculated by using the formula given in ASTM C215 [33] as,

$$E_d = CMn^2 \quad (2)$$

where M (kg) is the mass of the prism specimen, n (Hz) is the fundamental transverse resonant frequency and C (m^{-1}) is a parameter

that depends on the size, shape and the dynamic Poisson's ratio of the concrete specimen.

2.3.4. Poisson's ratio

Dynamic Poisson's ratios for the reactive and control concrete were estimated by measuring the pulse velocities of P- and S-waves in cube specimens (254 mm) by using a "Pundit Lab+" ultrasonic equipment from Proceq USA, Inc. Dynamic Poisson's ratio (μ_d) was calculated by using the formula given in Proceq [34] as,

$$\mu_d = \frac{V_p^2 - 2V_s^2}{2\left(V_p^2 - V_s^2\right)} \quad (3)$$

where V_p (m/s) and V_s (m/s) are the pulse velocities of P- and S-waves, respectively.

The values of μ_d were obtained as 0.276 and 0.267, respectively, for the reactive and non-reactive concrete specimens conditioned at 23 ± 3 °C for 6 months of casting. These values were used to calculate the dynamic modulus of elasticity of concrete by the resonant frequency method.

2.3.5. Damage rating index (DRI)

Damage Rating Index (DRI) method has emerged as a technique of quantifying the extent of damage in concrete [35]. The method was originally proposed by Grattan-Bellew in 1995 [24]; a revised version was proposed by Villeneuve et al. in 2012 [36], which was adopted in this study. Further reference was made to Sanchez et al. [23] and to the detailed guidelines on DRI published by Fournier et al. [37].

Two prisms were tested for DRI at each test age. For each prism, one slice near the middle and one slice near the end were taken and polished for the microscopic observation. The slices were prepared by successively polishing with diamond polishing pads and water to a surface roughness of approximately 5 μm. Forty-nine 1 cm^2 grids were prepared as shown in Fig. 1. Each grid was examined in a stereo binocular microscope at ~16× magnification to count the seven petrographic features as listed in Table 3. The numbers of counts were multiplied by the respective weighting factors and summed. The sum was normalized to an area of 100 cm^2 to provide the DRI value for a slice. DRI value for concrete at an age was obtained as the average for four slices from two prisms.

Fig. 1. Polished section of a concrete prism (age 3 months, CPT) for DRI analysis (each grid is 1 cm by 1 cm).

Table 3
Features counted in an individual grid as per the DRI method [36].

Petrographic features	Weighting factors
Closed/tight cracks in coarse aggregate particle	0.25
Opened cracks or network cracks in coarse aggregate particle	2
Cracks or network cracks with reaction product in coarse aggregate particle	2
Debonded coarse aggregate	3
Disaggregated/corroded aggregate particle	2
Cracks in cement paste	3
Cracks with reaction product in cement paste	3

3. Results and discussions

3.1. Expansion

Average longitudinal expansions of the concrete prisms in the CPT (38 °C) and ACPT (50 °C) are presented in Fig. 2. (The error bar in this and other figures in this paper represents one standard deviation). Since two prisms were destructively tested at different test dates, the number of prisms gradually decreased over time. Thus, each data point shown in the figure represents the average of a varying number of prisms. For the reactive concrete prisms tested under the CPT condition, the expansion at 14 days and 730 days represents the average of 18 prisms and four prisms, respectively. For the control concrete prisms tested under the CPT condition, the expansion at 28 days and 365 days represents the average of 12 and two prisms, respectively. For the reactive and control prisms tested under the ACPT condition, the expansion at 7 days and 187 days represents the average of nine and two prisms, respectively.

The ultimate expansion of control prisms for the CPT and ACPT conditions was less than 0.04%, a limit for non-reactivity as specified by ASTM C1293 [6]. For the CPT, the expansion of reactive concrete prisms was 0.23% in 365 days. It further increased to 0.26% in two years (730 days). For the ACPT, an expansion of 0.25% was observed in six months (187 days) for the reactive prisms. The total expansion and the trend of expansion for the reactive prisms were similar in both the CPT and ACPT; however, the rate of expansion was significantly faster in the ACPT as shown in Fig. 2.

Contrary to the literature [10,13,14], no reduction in expansion was observed due to the increase in temperature. One possible explanation could be that at 50 °C, the sulfate ions had minimal effect on reducing the pH of the concrete pore solution unlike at 60 °C at which the effect was reported as a possible reason for hav-

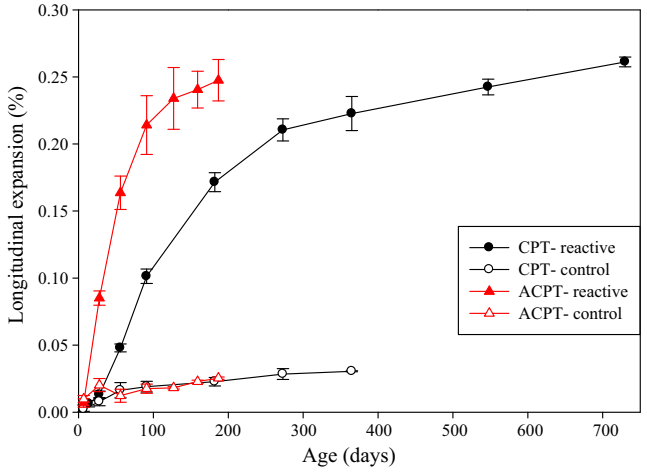

Fig. 2. Longitudinal expansion of concrete prisms in CPT and ACPT.

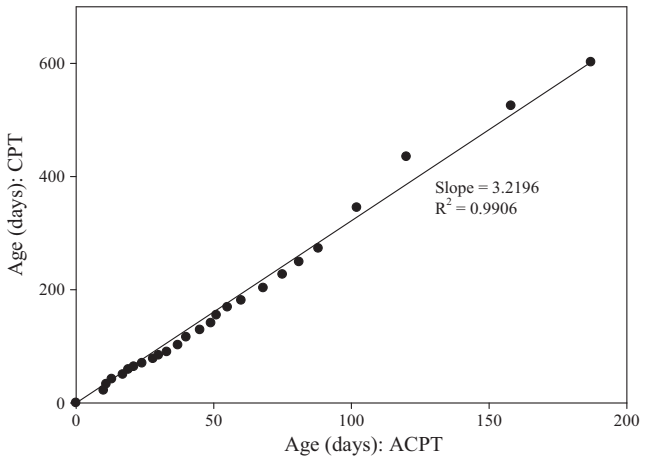

Fig. 3. Days required by reactive prisms in CPT and ACPT for identical expansion.

ing reduced expansion [10]. However, this phenomenon needs to be verified experimentally. Furthermore, in this study, the ACPT specimens were kept in sealed pails and the pails were stored inside a >95% relative humidity chamber. This would eliminate the effect of drying of prisms (drying of prisms was given as a possible reason for the reduced expansion at 60 °C [13,14]) compared to the tests in which pails are stored in relatively drier environment and the pails might not achieve perfectly sealed condition. Moreover, leaching has been an influencing factor for the expansion of concrete prism specimens [38] and its influence on ASR expansion at different temperatures may need further study.

Fig. 3 presents the days required by the reactive concrete for the identical expansions in the CPT and ACPT conditions. The number of days in the CPT and ACPT for identical expansions correlated with an R^2 value of 0.99. When the data was fit to a straight line passing through the origin, the slope of the line was 3.22, indicating that the rate of expansion in the ACPT was 3.22 times faster than in the CPT. The expansion vs. age data were re-plotted in Fig. 4 with different lower and upper horizontal scales for the ages for the CPT and ACPT, respectively, such that 3.22 days for the CPT corresponded to 1 day for the ACPT. When the scale for the ACPT was larger by a factor of 3.22 than in the CPT, the expansion curves from the CPT and ACPT overlapped. The expansion results suggest that the trend and the total expansion due to ASR remain unaffected by changing the accelerating temperature from 38 to 50 °C and the rate of expansion increases by 3.22 times.

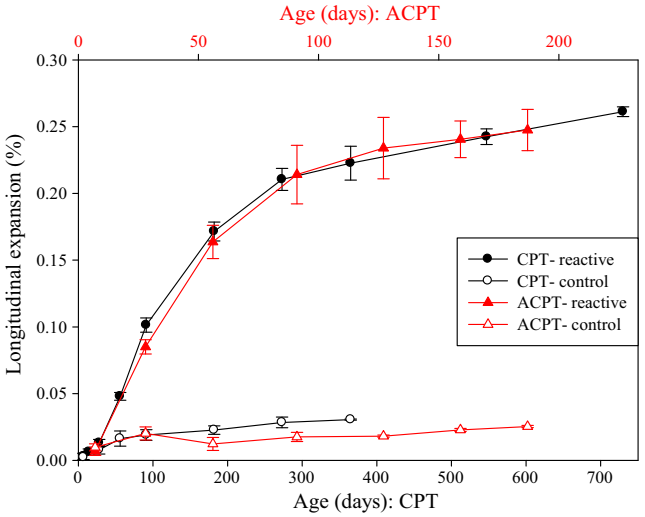

Fig. 4. Longitudinal expansion of concrete prisms in CPT and ACPT using different time scales (note: top horizontal scale for age of ACPT and bottom horizontal scale for age of CPT).

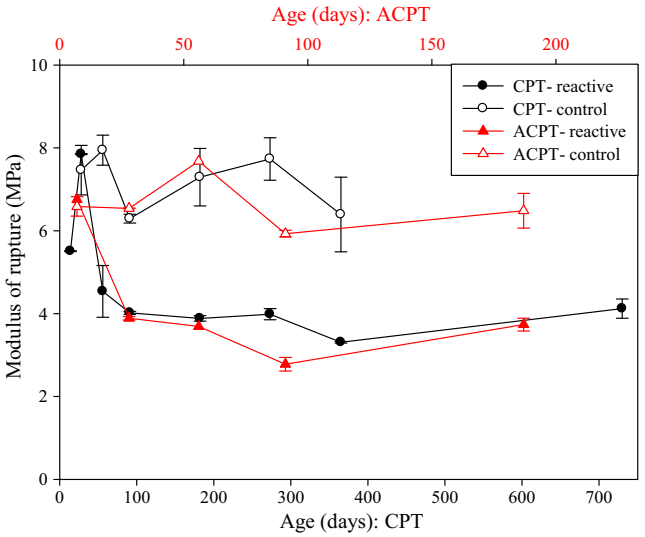

Fig. 5. Variation in modulus of rupture of concrete prism specimens over time using different time scales.

3.2. Modulus of rupture

Fig. 5 shows the modulus of rupture of concrete prism specimens for CPT and ACPT at different test ages. Each data point is an average for two prisms. The modulus of rupture for the control specimens varied between 6 and 8 MPa. Relatively larger scatter was observed in the control specimens than in the reactive specimens. This observation is consistent with [39], an experimental study that involved testing of several specimens. The study [39] showed that the coefficient of variation in modulus of rupture increases significantly with increasing flexural strength. Based on the finding of the study [39], ASTM standards for the flexural strength of concrete [32,40] mention that the coefficient of variation in modulus of rupture is dependent on the flexural strength of the specimens.

The modulus of rupture for the reactive prisms in CPT increased initially to attain its peak at 28 days. By 91 days, the modulus of rupture reduced to approximately 50% of its 28-day value. After 91 days, it reduced at a relatively slower rate until 365 days to reach 42% of its 28-day value. Closer examination of the data revealed that partial recovery of the property was observed from 365 to 730 days.

The modulus of rupture for the reactive specimens in the ACPT followed a similar trend as specimens in the CPT except that the trend occurred faster. The trend comprised of a sharp reduction in the modulus of rupture from 7 to 28 days, a relatively slower reduction from 28 to 91 days and a partial recovery from 91 to 187 days. The modulus of rupture at 28 days was 58% of its 7-day value and at 91 days, it was approximately 41% of its 7-day value. The modulus of rupture at 187 days was 55% of its 7-day value showing partial recovery from 91 to 187 days.

Partial recovery of the mechanical properties of ASR-affected concrete has also been observed in the literature [41–44]. A detailed explanation of the mechanism of partial recovery is reported by Gautam [45]. Irrespective of the underlying mechanism, an identical trend of partial recovery was observed in both CPT and ACPT specimens.

The reduction in the modulus of rupture appeared slightly greater in the ACPT specimens than in the CPT specimens. Based on the observed maximum value of modulus of rupture

(7.85 MPa), which occurred at 28 days in the CPT, and the observed minimum values (3.31 MPa in the CPT at 365 days and 2.78 MPa in the ACPT at 91 days), the modulus of rupture for the reactive concrete reduced by a maximum of 58% and 65% in the CPT and ACPT specimens, respectively.

3.3. Dynamic modulus of elasticity

Fig. 6 shows the dynamic modulus of elasticity for the prism specimens used in the CPT and the ACPT as calculated from the transverse resonant frequency test. Each data point is an average for two prisms. In order to illustrate the effect of ASR, the results in Fig. 6 are presented relative to the control prisms. The dynamic modulus of elasticity for the CPT specimens was normalized to the 28-day value of control prisms in the CPT. For the ACPT specimens, the dynamic modulus of elasticity was normalized to the 7-day value of control prisms in the ACPT. For the control prisms, the dynamic modulus of elasticity showed a slight and gradual increase over time. At 365 days, dynamic modulus of elasticity of the control prisms in the CPT increased by 5% compared to its 28-day value. Likewise, at 187 days, dynamic modulus of elasticity of the control prisms in the ACPT increased by 7% compared to its 7-day value. The slight and gradual increase in dynamic modulus of elasticity of control concrete must be due to the continued hydration of cement.

For the reactive concrete, the dynamic modulus of elasticity of the prisms in the CPT increased from 14 to 28 days and reduced thereafter until 273 days. The maximum reduction (18%) in the dynamic modulus of elasticity was observed at 273 days, with respect to the dynamic modulus of elasticity at 28 days. Partial recovery in the dynamic modulus of elasticity was observed from 273 to 365 days. In the ACPT specimens, the dynamic modulus of elasticity reduced by 12% from 7 to 28 days. The maximum reduction of 24% was observed at 56 days, with respect to the dynamic modulus of elasticity at 7 days. After 56 days, partial recovery was observed in the dynamic modulus of elasticity, a mechanism similar to that in the CPT specimens.

3.4. Damage rating index (DRI)

Table 4 presents the number of counts of the seven petrographic features for DRI per 100 grids for the reactive concrete specimens in both the CPT and the ACPT. The DRI value was calculated based on the number of counts by following the procedure outlined in Villeneuve et al. [36]. The DRI values for the reactive prisms in the CPT and ACPT are plotted against the longitudinal expansion as shown in Fig. 7. The DRI value increased with an increase in expansion and showed a fairly linear trend with expansion. Considering the relatively subjective nature of the DRI method, DRI results may be expected to incur larger variability compared to the expansion measurements.

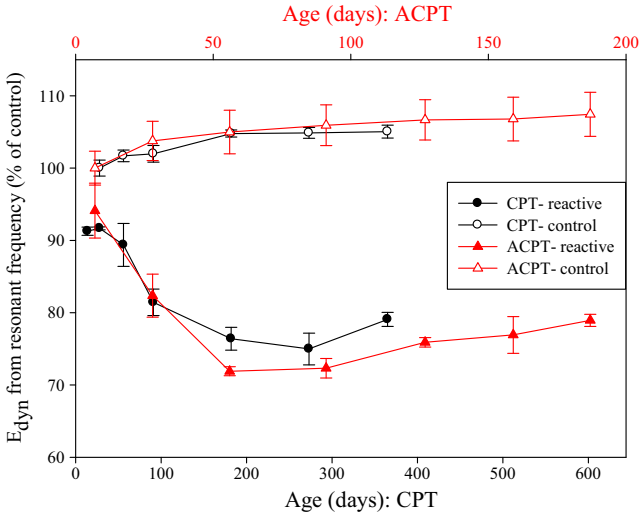

Fig. 6. Variation in dynamic modulus of elasticity over time (using different time scales) from the resonant frequency method.

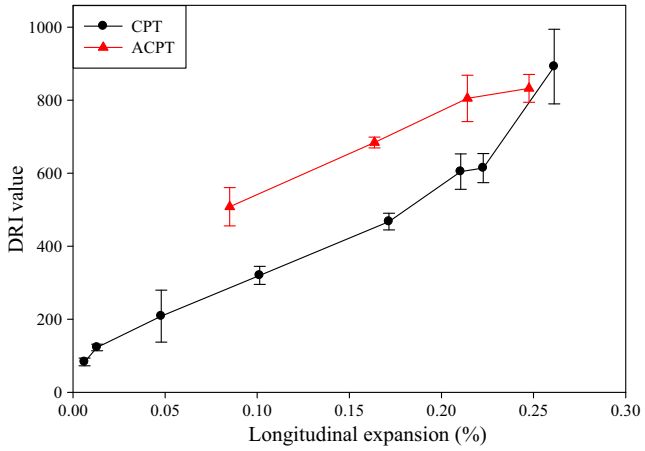

Fig. 7. DRI value versus longitudinal expansion for the reactive prisms in CPT and ACPT.

Table 4
Number of counts of the seven petrographic features per 100 cm^2.

Test	Age (days)	Exp. (%)	DRI value	Closed/tight cracks in coarse aggregates (1)	Opened cracks (or networks) (2)	Filled cracks (or networks) (3)	Debonded coarse aggregate (4)	Dis-aggregated/ corroded aggregate (5)	Cracks in cement paste (6)	Filled cracks in cement paste (7)	Sum (2 + 3 + 6 + 7)	Crack density (count/ cm^2)
CPT	14	0.006	83	148	3	15	3	1	0	0	18	0.18
	28	0.013	123	236	4	24	3	1	0	0	28	0.28
	56	0.048	209	273	16	48	2	1	2	0	66	0.66
	91	0.101	320	180	36	96	1	0	2	1	135	1.35
	182	0.171	468	197	22	153	2	1	17	4	196	1.96
	273	0.210	604	157	63	172	2	2	20	9	264	2.64
	365	0.223	614	125	66	166	1	2	23	14	269	2.69
	730	0.261	892	109	86	190	18	30	28	39	343	3.43
ACPT	28	0.085	508	182	31	167	3	7	12	3	213	2.13
	56	0.164	684	148	68	202	9	10	15	5	290	2.90
	91	0.214	805	141	88	231	6	11	24	6	349	3.49
	187	0.248	832	74	127	187	5	10	35	15	364	3.64

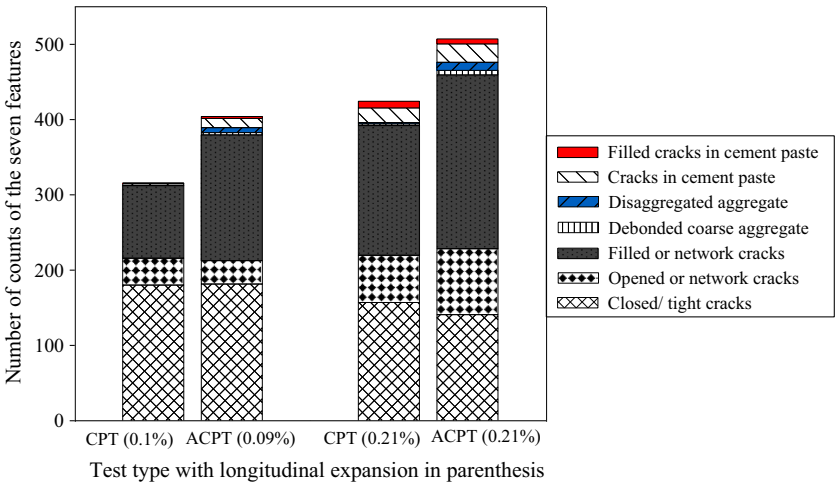

Fig. 8. Comparison of the number of counts (i.e. no weighting factors) of the damage features in CPT and ACPT (for 0.1 and 0.21% expansions).

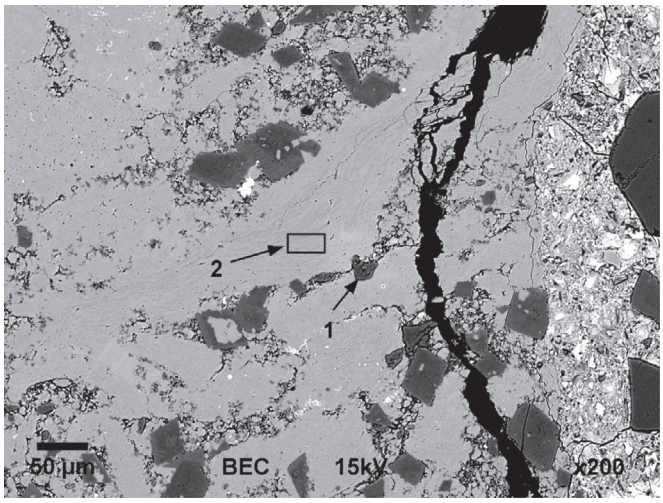

a) BSE image of a reactive aggregate particle undergoing ASR cracking. Two small areas "1" and "2" are located in the relatively darker silica and the relatively brighter calcite, respectively.

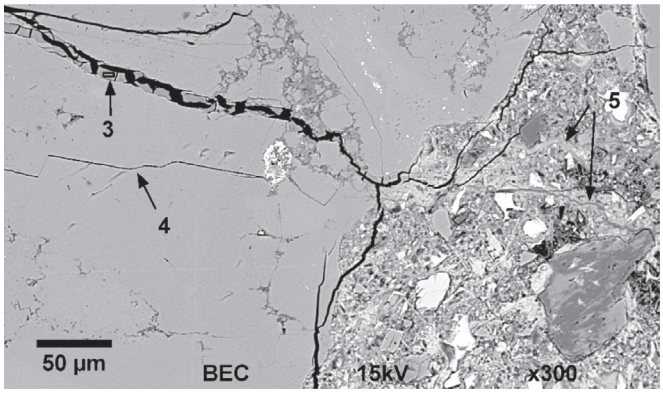

b) BSE image of an ASR crack continuing to the paste matrix. Label "3" shows ASR gel in a crack in an aggregate particle and label "4" shows a sharp crack in the aggregate particle. Label "5" shows the reaction product flown and diffused into the paste matrix.

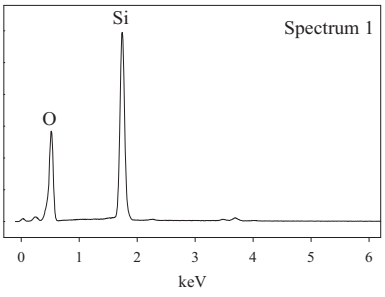

c) EDX spectrum of an area at "1"

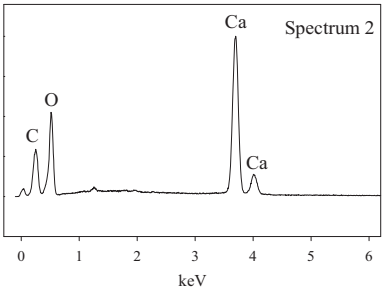

d) EDX spectrum of area "2"

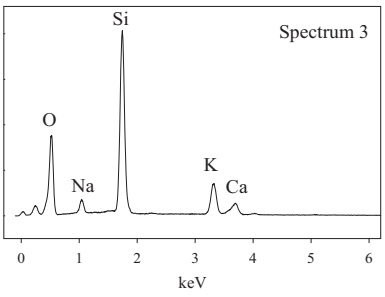

e) EDX spectrucm of area "3"

Fig. 9. SEM BSE images and EDX spectra of reactive aggregate and paste matrix in a concrete sample cured at 50 °C for 28 days.

3.4.1. Detailed discussion on the effect of elevated temperature

The DRI values were greater for the ACPT specimens than for the CPT specimens at the same expansion level as shown in Fig. 7. Until an expansion of 0.21%, the DRI value for the ACPT specimens was greater by approximately 200 than for the CPT specimens. Thereafter, despite a slower increase in expansion from 0.21% to 0.26%, the DRI value for the CPT specimens did indeed increase significantly. The DRI value for the CPT specimens approached closer to the ACPT specimens for an identical expansion value (Fig. 7). Debonding, disintegration of particles and paste cracks had an increased contribution to the DRI value for the CPT specimens corresponding to the increase in expansion from 0.21% (365 days) to 0.26% (730 days). The combined contribution of these features increased from 19% at 365 days to 35% at 730 days.

To further analyze whether greater DRI values in the ACPT actually indicated more cracks, the number of cracks without the weighting factors were compared. Fig. 8 compares the number of counts of the seven petrographic features in the CPT and ACPT for two different levels of expansion (~0.1% and 0.21%). For an identical expansion, the faster rate of reaction in the ACPT (compared to the CPT) induced more cracks in the aggregate particles. Also, for the expansion of ~0.1%, the number of paste cracks was greater in the ACPT specimens than in the CPT specimens.

In order to examine the process of cracking at the microscopic level, polished sections of concrete were prepared by using water-free processes and were examined under a scanning electron microscope (SEM). Fig. 9 shows backscattered electron (BSE) images and energy-dispersive X-ray spectroscopy (EDX) spectra of a sample taken from a concrete prism cured at 50 °C for 28 days. Fig. 9a shows a BSE image of a reactive aggregate particle undergoing ASR cracking and Fig. 9b shows an aggregate particle consisting of a crack with ASR product. The EDX spectrum of the ASR gel in the crack in Fig. 9b is shown in Fig. 9e. As shown in Fig. 9a, silica particles (EDX spectrum of which shown in Fig. 9c) are distributed inside the limestone aggregate (EDX spectrum for which shown in Fig. 9d). Cracking appears to initiate at the silica veins in which reactive silica (not all the silica is expected to be reactive) is attacked by alkali. The cracks are then widened to accommodate the expansive reactive alkali-silicate. The expansive pressure appears to break the aggregate and form some new and relatively sharper cracks as shown at location "4" in Fig. 9b. It is believed that formation of such new cracks is more likely in the ACPT specimens than in the CPT specimens. Furthermore, as shown at location "5" in Fig. 9b, once alkali-silicate is formed, it appears to flow and diffuse into the paste matrix. The alkali-silicate that was diffused in the paste matrix was seen to be associated with calcium and hence richer in calcium compared to the alkali silicate inside aggregate such as at location "3" in Fig. 9b [45]. It should be noted that ASR expansion at the macro level is contributed both by the discrete crack openings at the aggregate and paste matrix, and also as a result of the paste matrix expansion contributed by the swelling of the diffused reaction product.

To further reveal the mechanism at the microscopic level, Fig. 10 shows a digital microscope image of a polished surface of concrete cured at 50 °C for 91 days. An abundance of reaction product can be seen inside the aggregate particle. The pressure of the reaction product inside the aggregate is attributed to the cracking of the aggregate particle followed by paste cracking. This mechanism is in agreement with the cracking of the aggregate particles due to the expansive pressure of "gel pockets" and the propagation of cracking to the paste matrix as discussed by Dunant and Scrivener [46]. Moreover, the type of cracks in aggregate has been attributed to influencing the amount of paste cracking; "sharp" cracks in aggregate contribute to increased paste cracking [47]. The increased temperature of the ACPT is expected to result in the formation of an increased number of sharp cracks (e.g., location "4" in Fig. 9b) in aggregate particles, thus, resulting in extensive paste cracking before 91 days. A parameter called "crack density" was defined by Sanchez et al. [23] to better explain the cracking of concrete specimens due to ASR. Crack density is defined as the sum of the numbers of filled and opened cracks in aggregate and all the paste cracks per unit area of a polished surface of concrete. The crack density for the CPT and the ACPT specimens is shown in Table 4 which reveals that the ACPT resulted in a higher crack density and therefore a greater number of cracks compared to the specimens subjected CPT condition.

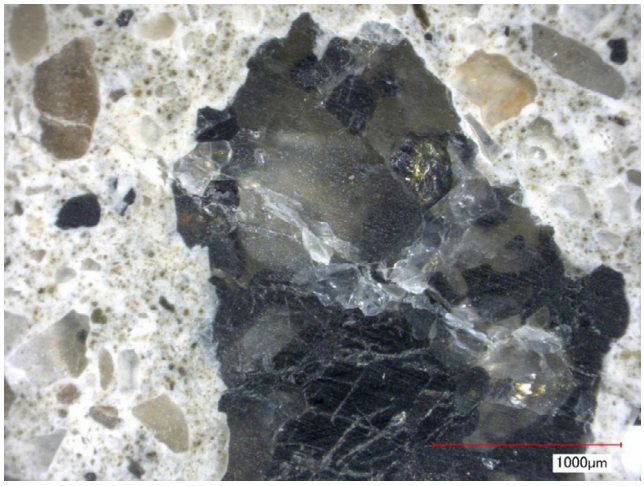

Fig. 10. Reaction product (white) in a coarse aggregate particle (grey to black) on a polished surface of concrete cured at 50 °C for 91 days, as observed under a digital microscope.

The relatively faster rate of reaction in the ACPT, analogous to a faster rate of loading, resulted in a greater number of cracks within the aggregate particles and a greater number of paste cracks at the moderate level of expansion of ~0.1% compared to the CPT. A recent numerical study [26] demonstrated that despite having identical expansion, the concrete conditioned at a higher temperature (50 °C) may experience more cracks compared to the concrete conditioned at a lower temperature (38 °C). Owing to the inherent heterogeneity of concrete and the viscoelastic behavior of the paste matrix, the response of concrete to expansive stresses varies as a function of the rate of stress application. As observed in this study, the paste (actually the mortar matrix) cracking followed the aggregate cracking. Once the reaction product swelled, it applied pressure to the mortar matrix, which in turn accommodated the pressure by either expanding or cracking. The rate of application of expansive pressure was influenced by the rate of reaction, which was markedly faster in the ACPT than in the CPT. Due to the viscoelastic nature of the matrix, the faster reaction (in the ACPT) resulted in increased paste cracking; in contrast, the relatively slower reaction (in the CPT) accommodated more expansive pressure through expansion by undergoing less paste cracking. Fig. 11 shows the contribution of aggregate cracks and paste cracks to the DRI value for different levels of expansion of specimens subjected to the CPT and ACPT. From Fig. 11, after having approximately 0.14% expansion of concrete, it is expected that the expansive pressure may markedly surpass the tensile strength of the matrix even in the CPT and results in increasing levels of paste cracking.

The prism surfaces that exhibited the most surface cracking were scanned in a flatbed scanner. A portion of the scanned images are shown in Fig. 12. The chosen surfaces are among the ones that exhibited the most surface cracking to naked eyes. The prism surface in ACPT in 6 months showed a visible network of hairline

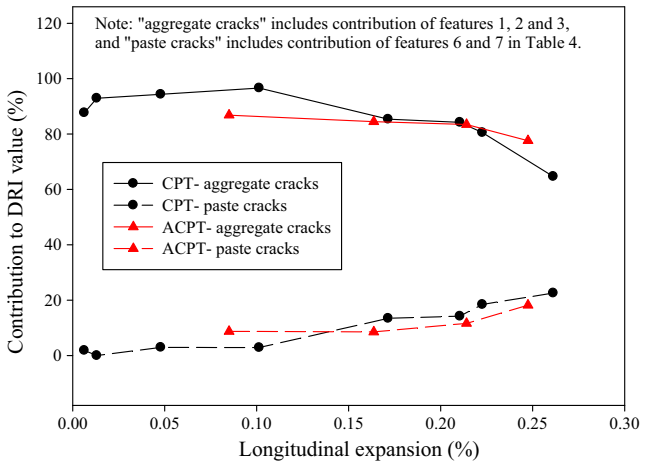

Fig. 11. Contributions of aggregate cracks and paste cracks to DRI value at different expansions for CPT and ACPT.

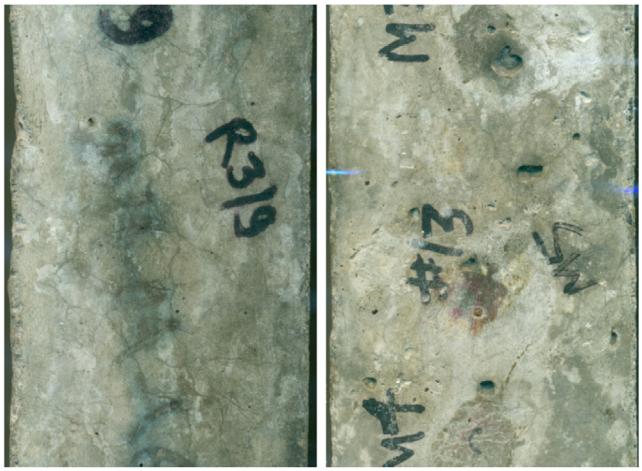

a) ACPT specimen after 6 months b) CPT specimen after 2 years

Fig. 12. Flatbed scan images of the middle portion of concrete prisms (width 75 mm). The a) prism in ACPT exhibited a visible network of cracks compared to the b) prism in CPT.

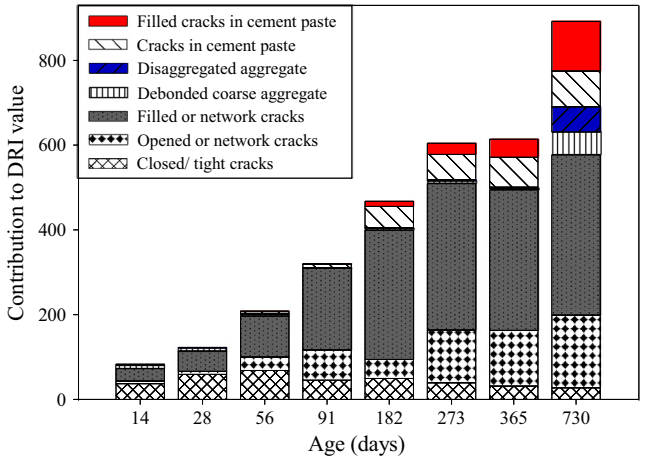

Fig. 13. DRI of reactive prisms in CPT at different ages with contributions of the seven petrographic features.

cracks. The prism surface in CPT in 2 years showed a few hairline cracks. These images suggest that an increase in temperature causes an increased cracking of the concrete microstructure.

3.4.2. Evolution of damage as measured by DRI method

The DRI method in this study was useful to understand the evolution of ASR damage in reactive concrete. Fig. 13 shows the evolution of the ASR damage with age as measured by the DRI method for the CPT specimens from 14 to 730 days.

The individual contributions of the seven petrographic features to the DRI value are shown in Fig. 13.The damage was initiated in the reactive aggregate particles. The contribution to DRI value was dominated by closed/tight cracks until 56 days (Fig. 13). The closed/tight cracks contributed up to 48% of the DRI value at 28 days but their contribution decreased significantly after 56 days. The number of counts of closed/tight cracks (Table 4) increased from 14 to 56 days but decreased thereafter indicating that damage initiation was predominantly in the form of closed/tight cracks in the aggregates. On the other hand, the number of counts of filled and opened cracks (Table 4) generally increased with an increase in age. An increase in the number of filled and opened cracks but a decrease in the number of closed/tight cracks indicates that most of the closed/tight cracks were the precursor of the filled or the opened cracks. Closed/tight cracks have been viewed as not only due to ASR, but also due to effects of aggregate weathering and/ or crushing operations prior to use in concrete [23,25,37]. However, the two types (ASR cracks or preexisting cracks) can be differentiated if DRI is examined in a reference concrete slice that is prepared before the evolution of ASR. For instance, even if aggregates had pre-existing closed/tight cracks, these were included in the number of counts at 14 days, which was 148 per 100 cm^2 (Table 4). After multiplying the number of counts with the corresponding weighting factor of 0.25, the maximum possible contribution of such cracks was thus limited to a DRI value of 37. Had a slice been prepared at the age of one day, the number of closed/tight cracks must have been even lower. The "closed/tight cracks" petrographic feature indeed serves as an important parameter to capture the onset of damage due to ASR.

The contribution to DRI value was dominated by the aggregate cracks throughout the study duration. The closed/tight cracks gradually transformed into filled or opened cracks. The paste cracks were insignificant until 91 days in the CPT indicating that they initiated only after a significant reaction took place in the aggregate particles. Fig. 11 shows the contribution of aggregate cracks and paste cracks to the DRI value for different levels of prism expansion subjected to the CPT and ACPT conditions. The contribution and its trend appear identical in both cases except that paste cracking is pronounced in the ACPT specimens even at a moderate expansion, of say 0.1%. The contribution of aggregate cracks varied from 96% to 64% to dominate the DRI value. The contribution of paste cracks gradually increased from 0% to a maximum of 23%.

3.4.3. Some remarks on the DRI method

The DRI is a comprehensive method to quantitatively determining the degree of damage due to ASR. Researchers have reported some limitations of the DRI method [23,36,37]. First, the method is a semi-quantitative method that can have a large variability on the results based on the experience of an operator. In order to reduce the variability between operators in the DRI method, Villeneuve et al. [36] proposed a revision in the definition of the damage features and in their weighting factors. Second, even though the weighting factors were chosen in a logical basis, the relative weights assigned to several damage features are still arbitrary [23]. Third, the DRI value can have high variability based on the minimum size of the aggregate particle that is accounted for counting the damage features. A minimum size of 2 mm has been recommended by Fournier et al. [37], and later by Sanchez et al. [48] as 1 mm.

Furthermore, this study highlights three additional limitations, particularly in the context of characterizing the evolution of

damage, including: the ambiguity associated with the thickness of a crack in classifying it as either tight or opened crack; the length of cracks; and the coalescence of multiple cracks into a single damage feature of disaggregated particle. These three aspects are discussed further.

i) Classification of an aggregate crack as a closed/tight crack or a filled or an opened crack is based on the judgment of the operator as to the crack thickness. Many closed/tight cracks grow in width and become transformed into filled or opened cracks. A polished surface of concrete at a particular instance in time would reveal cracks with a wide range of thicknesses and also cracks with varying thickness along their length. This can result in an ambiguous situation whereby a particular crack may be classified either as a closed/tight crack or a filled or an opened crack.
ii) This study reveals that the length of cracks is as an important aspect that is not currently sufficiently considered in the DRI method. While an aggregate particle less than 2 mm on the polished section is not included in crack counting [37], there are many instances of short cracks (1–2 mm long) in larger particles. Such a short crack receives the same weighting in the calculation of a DRI value as by a 14 mm long crack (which is approximately the diagonal dimension of a 1 cm^2 grid) if the crack is contained within one grid. Also, two or three cracks of length, say 3 mm, at one stage of reaction could ultimately grow to form a single long crack, say 10–14 mm long, at a later stage. Depending on when the concrete slice is made, initially a particular damage feature may be counted as three cracks but its mature form could be counted as a single crack.
iii) A number of relatively smaller filled or opened cracks would be counted as multiple discrete cracks at an early age, but later would coalesce into a reacted fraction of an aggregate, and therefore be counted as a single disaggregated particle. Although both features have the same weighting in the calculation of a DRI value, initially a particular damage feature may be counted as multiple cracks but its mature form could be counted as a single disaggregated particle.

The discrepancy in DRI corresponding to the identical expansions in the CPT and ACPT specimens (as discussed in Section 3.4.1 and shown in Fig. 8) could partly be attributed to these three limitations. For instance, the elevated temperature in the ACPT resulted in several smaller cracks as suggested by greater total number of aggregate cracks (sum of the crack counts in columns 1, 2 and 3 of Table 4) in the ACPT specimens than in the CPT specimens for similar levels of expansion. However, some of the smaller cracks coalesced to form larger cracks, and this was more so in the ACPT specimens as suggested by a decrease in the total number of aggregate cracks from 459 to 388 during 91–187 days.

4. Summary and concluding remarks

This study investigated the influence of elevated conditioning temperature on the damage caused by ASR on reactive concrete containing reactive Spratt as the coarse aggregate. Two sets of tests were performed, namely 1) conditioning specimens in accordance with the concrete prism test (CPT) performed at 38 °C and 2) conditioning specimens in accordance with the accelerated concrete prism test (ACPT) performed at 50 °C.

With an increase of 12 °C temperature from 38 to 50 °C, the expansion of the ACPT specimens was 3.22 times faster than of the CPT specimens. Except for the rate of expansion, the overall trend of expansion and the ultimate expansion were similar for both the ACPT and CPT specimens.

Accounting for the 3.22 times faster rate of reaction in the ACPT specimens than in the CPT specimens, the trends of reduction and partial recovery in modulus of rupture and in dynamic modulus of elasticity were identical in both CPT and ACPT specimens. However, the reduction was slightly greater in the ACPT specimens than in the CPT specimens.

DRI results elucidated the evolution of damage due to ASR in the reactive concrete. The ability of the DRI method to account for fine cracks captured the onset of damage due to ASR. Despite some limitations, DRI is a comprehensive method for investigating the damage due to ASR. The individual petrographic features of the DRI method are instrumental to understand the evolution of damage due to ASR. The faster rate of reaction in the ACPT induced greater number of cracks at earlier stages of the reaction. This resulted in a larger DRI value of the ACPT specimens than of the CPT specimens with identical expansion. While the expansive pressure of a relatively slower reaction was accommodated by the CPT specimens without undergoing significant paste cracking, after having approximately 0.14% concrete expansion, the expansive pressure markedly surpassed the tensile strength of the matrix and caused increased levels of paste cracking. On the other hand, some smaller cracks in the ACPT coalesced to form larger cracks, particularly from 91 to 187 days.

Identical expansions and similar trends of the reactive concrete's modulus of rupture and dynamic modulus of elasticity suggest that an increase in conditioning temperature from 38 °C to 50 °C speeds up the test with little effect on the ASR mechanism based on specimens in this study. Nevertheless, a slight increase in the extent of damage and microstructural cracking with a 12 °C rise in temperature indicates that while accelerated tests are necessary for ASR studies, an increased temperature is likely to involve an increased deviation in the response of concrete from that in the field concrete structures, which was, however, not investigated in this study. A similar study in the future for a broader range of reactive aggregates and conditioning temperatures will elaborate the understanding of the effect of temperature on the ASR performance of concrete.

Acknowledgements

The authors acknowledge the funding provided through a contract by Canadian Nuclear Safety Commission (CNSC). However, the contents of this study do not represent, in any case, the technical position of the CNSC. We also acknowledge the Ministry of Transportation Ontario, Canada for providing the reactive Spratt aggregate; Lafarge Canada Inc. for providing the non-reactive Orillia sand; Dufferin Construction Company, Ontario, Canada for providing the non-reactive coarse aggregate; and Holcim Canada Inc. for providing the cement. We thank Prof. Karl Peterson for his support in microscopic analysis.

References

[1] J.W. Pan, Y.T. Feng, J.T. Wang, Q.C. Sun, C.H. Zhang, D.R.J. Owen, Modeling of alkali-silica reaction in concrete: a review, Front. Struct. Civ. Eng. 6 (2012) 1–18.
[2] R.D. Hooton, C. Rogers, C.A. MacDonald, T. Ramlochan, Twenty-year field evaluation of alkali-silica reaction mitigation, ACI Mater. J. 110 (2013) 539–548.
[3] S. Multon, J.F. Seignol, F. Toutlemonde, Structural behavior of concrete beams affected by alkali-silica reaction, ACI Mater. J. 102 (2005) 67–76.
[4] R. Martin, J. Renaud, S. Multon, F. Toutlemonde, Structural behavior of plain and reinforced concrete beams affected by combined AAR and DEF, in: 14th Int. Conf. Alkali Aggreg. React., Texas, 2012.
[5] E.R. Giannini, Evaluation of concrete structures affected by alkali-silica reaction and delayed ettringite formation (Ph.D. thesis), The University of Texas at Austin, 2012.

[6] ASTM C1293, Standard Test Method for Determination of Length Change of Concrete Due to Alkali-Silica Reaction, ASTM International, West Conshohocken, PA, 2015.
[7] CSA A23.2-14A, Potential Expansivity of Aggregates (Procedure for Length Change Due to Alkali-Aggregate Reaction in Concrete Prisms at 38 °C), CSA Group, Mississauga, ON, Canada, 2015.
[8] RILEM TC 106-AAR, Detection of potential alkali-reactivity of aggregates - method for aggregate combinations using concrete prisms, Mater. Struct. 33 (2000) 290–293.
[9] R. Ranc, L. Debray, Reference test methods and a performance criterion for concrete structures, in: 9th Int. Conf. Alkali-Aggregate React. Concr., The Concrete Society, London, U.K., 1992, pp. 110–116.
[10] B. Fournier, R. Chevrier, M. de Grosbois, R. Lisella, K.J. Folliard, J.H. Ideker, et al., The accelerated concrete prism test (60 °C): variability of the test method and proposed expansion limits, in: 12th Int. Conf. Alkali Aggreg. React., Beijing, 2004, pp. 314–323.
[11] M.D.A. Thomas, B. Fournier, K.J. Folliard, J.H. Ideker, M.H. Shehata, Test methods for evaluating preventive measures for controlling expansion due to alkali–silica reaction in concrete, Cem. Concr. Res. 36 (2006) 1842–1856.
[12] RILEM TC 219-ACS, RILEM Recommended Test Method AAR-4.1, Detection of Potential Alkali-Reactivity – 60 °C Test Method for Aggregate Combinations Using Concrete Prisms (Draft) Bagneux, France, 2011.
[13] K.J. Folliard, J.H. Ideker, M.D.A. Thomas, B. Fournier, Assessing aggregate reactivity using the accelerated concrete prism test, in: V.M. Malhotra (Ed.), 7th CANMET/ACI Int. Conf. Recent Adv. Concr. Technol., Las Vegas, 2004, pp. 269–283.
[14] J.H. Ideker, B.L. East, K.J. Folliard, M.D.A. Thomas, B. Fournier, The current state of the accelerated concrete prism test, Cem. Concr. Res. 40 (2010) 550–555.
[15] F.-J. Ulm, O. Coussy, L. Kefei, C. Larive, Thermo-chemo-mechanics of ASR expansion in concrete structures, J. Eng. Mech. 233–242 (2000).
[16] R. Helmuth, D. Stark, S. Diamond, M. Moranville-regourd, Alkali-Silica Reactivity: An Overview of Research, National Research Council, Washington DC, USA, 1993.
[17] X. Lingling, D. Min, L. Xianghui, Inhibition of fly ash on the alkali silica reaction (ASR) in concrete with alkali-reactive sandstone as aggregate, in: 14th Int. Conf. Alkali Aggreg. React., Texas, 2012.
[18] C. Larive, Combined contribution of experiments and modelling to the understanding of alkali-aggregate reaction and its mechanical consequences (Ph.D. thesis; in: French), Ecole Nationale des Ponts et Chausses, 1998.
[19] M. Ben Haha, Mechanical Effects of Alkali Silica Reaction in Concrete Studied by SEM-Image Analysis, Ecole Polytechnique federale De Lausanne, 2006.
[20] N. Orbovic, D.K. Panesar, S.A. Sheikh, F.J. Vecchio, C.-P. Lamarche, A. Blahoianu, Alkali aggregate reaction in nuclear concrete structures: Part 1: a holistic approach, in: SMiRT23, Manchester, U.K., 2015.
[21] P. Rivard, B. Fournier, G. Ballivy, The damage rating index method for ASR affected concrete – a critical review of petrographic features of deterioration and evaluation criteria, Cem. Concr. Aggregates 24 (2002) 1–11.
[22] P. Rivard, G. Ballivy, Assessment of the expansion related to alkali-silica reaction by the damage rating index method, Constr. Build. Mater. 19 (2005) 83–90.
[23] L.F.M. Sanchez, B. Fournier, M. Jolin, J. Duchesne, Reliable quantification of AAR damage through assessment of the damage rating index (DRI), Cem. Concr. Res. 67 (2015) 74–92.
[24] P.E. Grattan-Bellew, Laboratory evaluation of alkali-silica reaction in concrete from Saunders Generating Station, ACI Mater. J. 92 (1995) 126–133.
[25] L. Sanchez, Contribution to the assessment of damage in aging concrete infrastructures affected by alkali-aggregate reaction (Ph.D. thesis), Laval University, 2014.
[26] A.B. Giorla, K.L. Scrivener, C.F. Dunant, Influence of visco-elasticity on the stress development induced by alkali–silica reaction, Cem. Concr. Res. 70 (2015) 1–8.
[27] ASTM C1260, Standard Test Method for Potential Alkali Reactivity of Aggregates (Mortar-Bar Method), ASTM International, West Conshohocken, PA, 2014.
[28] B. Fournier, C.A. Rogers, C. MacDonald, Multilaboratory study of the concrete prism and accelerated mortar bar expansion tests with Spratt aggregate, in: 14th Int. Conf. Alkali Aggreg. React., Texas, USA, 2012, p. 10.
[29] B. Fournier, C. Rogers, Multi-laboratory study of accelerated mortar bar test and concrete prism expansion tests at 38° and 60 °C, in: 13th Int. Conf. Alkali Aggreg. React. Concr., Trondheim, Norway, 2008.
[30] M.D.A. Thomas, K.J. Folliard, B. Fournier, G. Ahlstrom, A prescriptive specification for the selection of measures for preventing alkali-silica reaction, in: 14th Int. Conf. Alkali Aggreg. React., Texas, 2012.
[31] C.A. Rogers, C.A. MacDonald, The geology, properties and field performance of alkali-aggregate reactive Spratt, Sudbury and Pittsburg aggregate distributed by the Ontario Ministry of Transportation, in: 14th Int. Conf. Alkali Aggreg. React., Texas, USA, 2012, p. 10.
[32] ASTM C78, Standard Test Method for Flexural Strength of Concrete (Using Simple Beam with Third-Point Loading), ASTM International, West Conshohocken, PA, 2015.
[33] ASTM C215, Standard Test Method for Fundamental Transverse, Longitudinal, and Torsional Resonant Frequencies of Concrete Specimens, ASTM International, West Conshohocken, PA, 2008.
[34] Proceq, Operating Instructions: Shear Wave Transducers 250 kHz, 2013, pp. 1–4.
[35] P.E. Grattan-Bellew, Petrographic methods for distinguishing between alkali-silica, alkali-carbonate reactions and other mechanisms of concrete deterioration, in: 14th Int. Conf. Alkali Aggreg. React., Texas, 2012, p. 10.
[36] V. Villeneuve, B. Fournier, J. Duchesne, Determination of the damage in concrete affected by ASR – the damage rating index (DRI), in: 14th Int. Conf. Alkali Aggreg. React. Concr., Texas, USA, 2012, p. 10.
[37] B. Fournier, P.-L. Fecteau, V. Villeneuve, S. Tremblay, L.F.M. Sanchez, Description of Petrographic Features of Damage in Concrete Used in the Determination of the Damage Rating Index (DRI), Laval University, Quebec City, Quebec, Canada, 2015.
[38] S. Multon, A. Sellier, Multi-scale analysis of alkali-silica reaction (ASR): impact of alkali leaching on scale effects affecting expansion tests, Cem. Concr. Res. 81 (2016) 122–133, http://dx.doi.org/10.1016/j.cemconres.2015.12.007.
[39] P.M. Carrasquillo, R.L. Carrasquillo, Improved Concrete Quality Control Procedures Including Third Point Loading, Center For Transportation Research, The University of Texas at Austin, Texas, 1987.
[40] ASTM C293, Standard Test Method for Flexural Strength of Concrete (Using Simple Beam with Center-Point Loading), ASTM International, West Conshohocken, PA, 2010.
[41] T. Ahmed, E. Burley, S. Rigden, A.I. Abu-Tair, The effect of alkali reactivity on the mechanical properties of concrete, Constr. Build. Mater. 17 (2003) 123–144.
[42] R.N. Swamy, M.M. Al-Asali, Engineering properties of concrete affected by alkali-silica reaction, ACI Mater. J. 367–374 (1988).
[43] F. Bektas, K. Wang, Performance of ground clay brick in ASR-affected concrete: effects on expansion, mechanical properties and ASR gel chemistry, Cem. Concr. Compos. 34 (2012) 273–278.
[44] H. Kagimoto, Y. Yasuda, M. Kawamura, ASR expansion, expansive pressure and cracking in concrete prisms under various degrees of restraint, Cem. Concr. Res. 59 (2014) 1–15.
[45] B.P. Gautam, Multiaxially loaded concrete undergoing alkali-silica reaction (ASR) (Ph.D. thesis), University of Toronto, 2016.
[46] C.F. Dunant, K.L. Scrivener, Micro-mechanical modelling of alkali–silica-reaction-induced degradation using the AMIE framework, Cem. Concr. Res. 40 (2010) 517–525.
[47] L.F.M. Sanchez, S. Multon, A. Sellier, M. Cyr, B. Fournier, M. Jolin, Comparative study of a chemo–mechanical modeling for alkali silica reaction (ASR) with experimental evidences, Constr. Build. Mater. 72 (2014) 301–315.
[48] L. Sanchez, B. Fournier, M. Jolin, M.A.B. Bedoya, J. Bastien, J. Duchesne, Use of damage rating index to quantify alkali-silica reaction damage in concrete: fine versus coarse aggregate, ACI Mater. J. 113 (2016) 395–407.